**Applied Coastal Research and Engineering, Inc.**
766 Falmouth Road
Suite A-1
Mashpee, MA 02649

## MEMORANDUM

**Date:** **April 29, 2008**

**To:** **U.S. Army Corps of Engineers, New England District**

**From:** **Sean Kelley, P.E. and John Ramsey, P.E.**

**Subject:** **Hydrodynamic Model of Chatham Harbor/Pleasant Bay including 2007 North Breach**

### 1. INTRODUCTION

An updated hydrodynamic analysis of the Pleasant Bay estuary was performed to determine the present state of the system since the formation of the north beach breach during the April 2007 Patriot's Day northeast storm. For the purposes of this memo, the time period after the north beach breach will be referred to as "post-breach". The hydrodynamics of the post-breach system were also compared to 2004 pre-breach conditions, using data and model results from the Massachusetts Estuaries Project report of Pleasant Bay (Howes *et al*., 2006).

For the post-breach analysis, Applied Coastal relied on data assembled from a variety of sources. LIDAR bathymetry and topography data from the New England District of the U.S. Army Corps of Engineers (USACE) were made available from two separate surveys flown in April and October 2007. Tide data from established gauge stations at the Chatham Fish Pier (station T2 indicated in Figure 1, maintained by the Town of Chatham Department of Health and Environment) and Meetinghouse Pond (station T3 in Figure 1, maintained by the Provincetown Center for Coastal Studies) were also made available.

To supplement available data from other sources, additional tide and Acoustic Doppler Current Profiler (ADCP) data were collected as part of this study. Tide data were collected in November 2007 at a station located offshore Nauset Beach (T1 in Figure 1), between the two inlets. An ADCP survey of currents was conducted on November 14, 2007. The ADCP survey was designed to measure the flow through each inlet during a single tide cycle. Two cross-channel transects (A1 and A2 shown in Figure 1) were followed during the course of the survey.

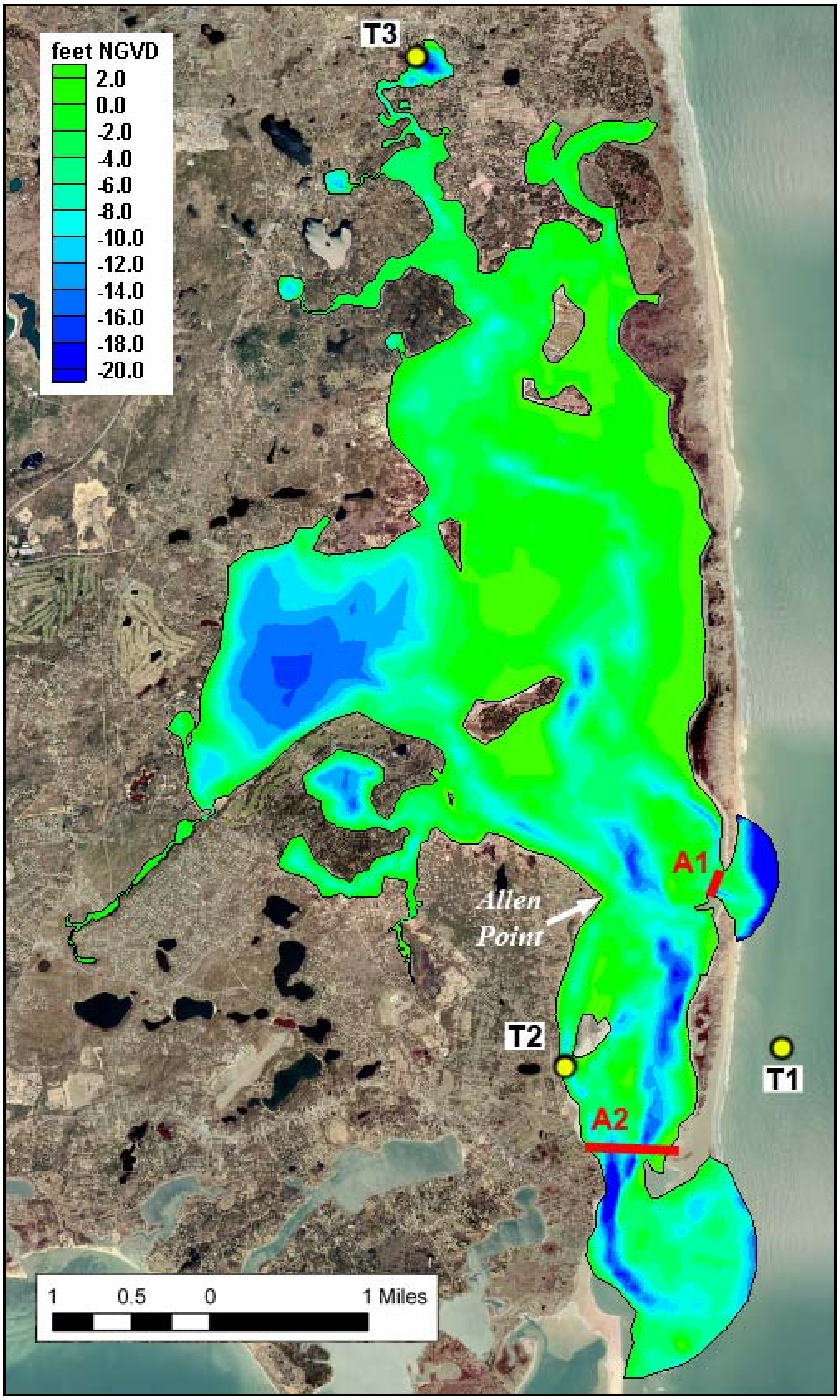


Figure 1. Plot of Pleasant Bay bathymetry, with tide stations (T1 through T3) and ADCP survey transects (A1 and A2).

## 2. DATA PROCESSING AND ANALYSIS

The bathymetry, tide and ADCP data were processed to provide the necessary baseline information to develop, calibrate and verify the hydrodynamic model of post-breach Pleasant Bay. A detailed description of the analysis techniques applied to the data utilized in this study can be found in the Pleasant Bay MEP report (Howes *et al*., 2006).

### 2.1 LIDAR Bathymetry

The LIDAR bathymetry data from the USACE were culled to reduce the number of data points and to make the files more manageable. A simple computer code was written to select every twentieth point of each data file from the surveys. The resulting sub-sets of the original files still provided more-than-ample data density for use in the development of the hydrodynamic model. The vertical datum of the bathymetry data was then converted from NAVD to NGVD, to be consistent with the prior MEP Pleasant Bay study.

### 2.2 Tide Data

A harmonic analysis of the tide data collected in 2007 (Figure 2) at the three stations was performed to determine the amplitude of the eight constituents listed in Table 1. The period between November 8 and 30, 2007 was used for this analysis since it was the maximum length of time of concurrent data from the three stations. The offshore gauge was deployed between these dates. The gauges at the fish pier and Meetinghouse Pond have longer records. The Meetinghouse Pond data were recorded using a 6 minute sampling period, and were re-sampled using a 10 minute period for the harmonic analysis and for the model calibration. The computed constituent amplitudes are shown for both the recent 2007 deployment period, and the earlier 2004 deployment for the MEP study.

The two time periods are roughly comparable, though there is a 0.18 foot difference in the $M_2$ amplitude (which is one-half the total range of the $M_2$ lunar semi-diurnal tide constituent) between the 2004 and 2007 data. Some variation is expected since both periods are relatively short. Tidal constituents computed for the purpose of tide prediction by agencies such as NOAA are computed typically using a complete tidal epoch of 19-years. Though the difference in constituent amplitudes in part is due to a bias from the different sampling periods, some of the increase seen at the Fish Pier and at Meetinghouse Pond is due to the opening of the north breach. The $M_2$ amplitude increased 0.56 feet (i.e., a 1.12 foot total increase in range) at the Chatham Fish Pier and 0.27 feet (0.54 foot range increase) at Meetinghouse pond.

The total change in the tidal range between 2004 and 2007 is also evident by the computation of the standard tidal datums. Table 2 shows the tide datums computed using the same records used in the tidal harmonic analysis. The offshore ranges (i.e., difference between MWH and MLW) between 2004 and 2007 are comparable, at 6.7 feet and 7.3 feet respectively. The range at the fish pier increased from 4.3 feet to 5.6 feet. At Meetinghouse Pond the range increase was 0.7 feet, from 4.0 feet in 2007 to 4.7 in 2007.

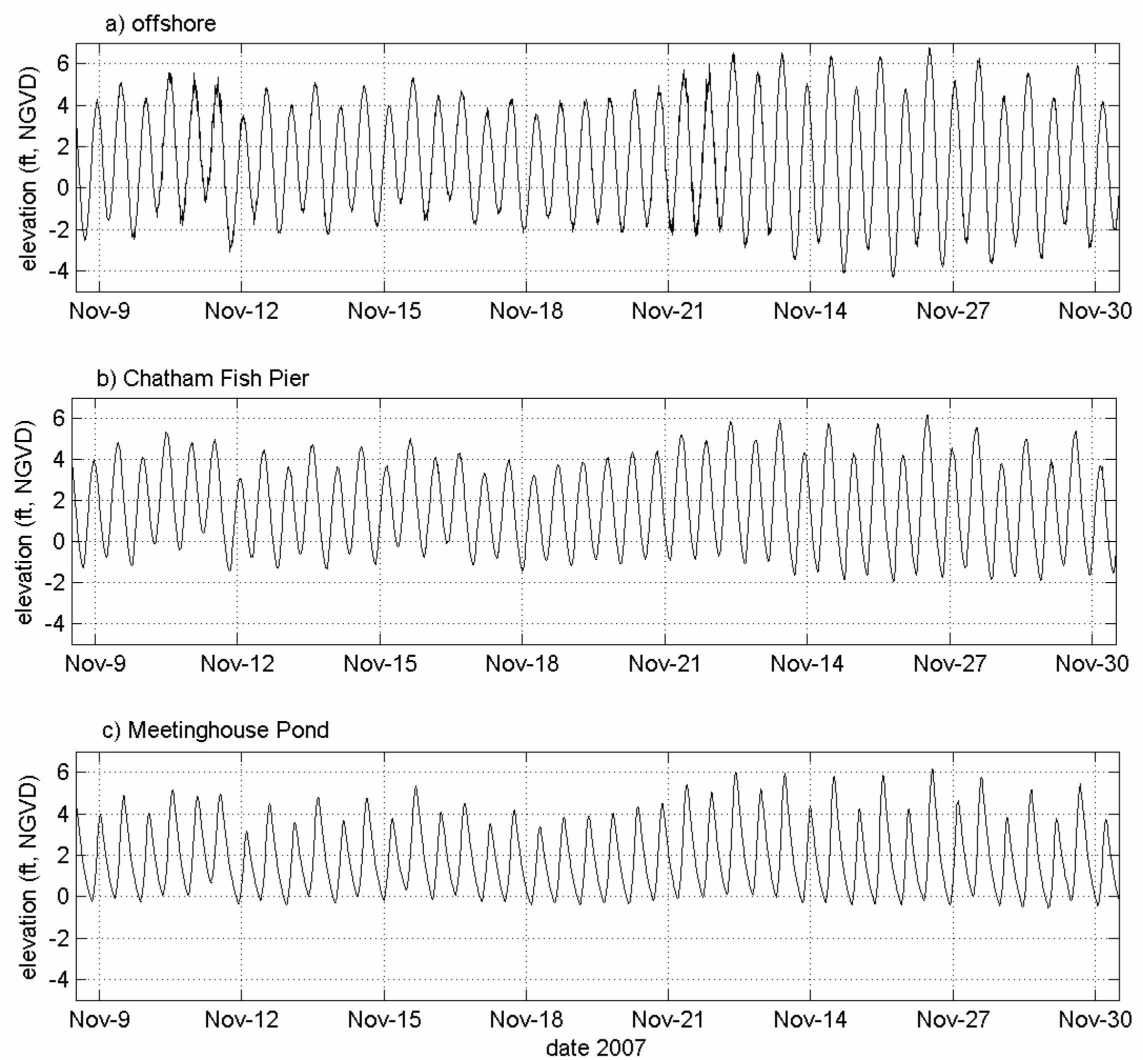


Figure 2. Measured tide during the November 2007 offshore gauge deployment period.

Table 1. Major tidal constituents determined for gauge locations in Pleasant Bay, for 2004 pre-breach and 2007 post-breach measurement periods

| | Amplitude (feet) | | | | | | | |
|---|---|---|---|---|---|---|---|---|
| Constituent | $M_2$ | $M_4$ | $M_6$ | $S_2$ | $N_2$ | $K_1$ | $O_1$ | $M_{sf}$ |
| Period (hours) | 12.42 | 6.21 | 4.14 | 12.00 | 12.66 | 23.93 | 25.82 | 354.61 |
| October 19 through November 30, 2004 | | | | | | | | |
| Offshore | 3.12 | 0.02 | 0.01 | 0.52 | 0.67 | 0.45 | 0.42 | 0.05 |
| Chatham Fish Pier | 2.03 | 0.08 | 0.06 | 0.27 | 0.39 | 0.33 | 0.29 | 0.06 |
| Meeting House Pond | 1.72 | 0.14 | 0.06 | 0.22 | 0.32 | 0.31 | 0.28 | 0.07 |
| November 8 through November 30, 2007 | | | | | | | | |
| Offshore | 3.30 | 0.03 | 0.01 | 0.47 | 0.93 | 0.49 | 0.46 | 0.08 |
| Chatham Fish Pier | 2.59 | 0.14 | 0.07 | 0.31 | 0.65 | 0.38 | 0.39 | 0.22 |
| Meeting House Pond | 1.99 | 0.49 | 0.09 | 0.23 | 0.49 | 0.35 | 0.36 | 0.20 |

| Tide Datum | Offshore | Fish Pier | Meeting-house Pond |
|---|---|---|---|
| **Table 2. Tide datums computed using data collected in the Pleasant Bay system in 2004 (pre-breach) and 2007 (post-breach). Datum elevations are given in feet relative to NGVD 29.** | | | |
| 2004 | | | |
| Maximum Tide | 6.8 | 5.5 | 5.4 |
| MHHW | 5.2 | 4.4 | 4.5 |
| MHW | 4.8 | 4.0 | 4.1 |
| MTL | 1.4 | 1.8 | 2.1 |
| MLW | -1.9 | -0.3 | 0.1 |
| MLLW | -2.4 | -0.5 | -0.0 |
| Minimum Tide | -3.7 | -1.2 | -0.4 |
| 2007 | | | |
| Maximum Tide | 6.8 | 6.1 | 6.2 |
| MHHW | 5.5 | 5.0 | 5.1 |
| MHW | 5.0 | 4.5 | 4.6 |
| MTL | 1.4 | 1.7 | 2.2 |
| MLW | -2.3 | -1.1 | -0.1 |
| MLLW | -2.7 | -1.3 | -0.3 |
| Minimum Tide | -4.3 | -1.9 | -0.5 |

### 2.3 ADCP data

An ADCP survey of tidal currents was conducted on November 14, 2007 to provide data for an independent verification of the hydrodynamic model's calibration. An ADCP measures water velocities (i.e., magnitude and direction relative to magnetic north) at discrete depths through the water column. For this survey, the ADCP sampled velocities every 0.82 feet (0.25 meter) from the surface to the bottom. With the ADCP fixed to a gimbaled mount attached to the gunwale of a boat, water column velocities can be record also at points across a channel as the boat navigates through the water.

The velocity data from each transect are used then to compute flow through the channel at discrete points in time. For the two transects followed in this survey, measurements were taken hourly, through maximum flood and ebb flows of a single tide cycle. At the north inlet, the maximum measured flood velocity was 6.0 ft/sec, 4.2 feet below the surface; and the maximum measured ebb velocities was 4.7 ft/sec, also 4.2 feet below the surface. At the south inlet, the maximum measured flood velocity was 4.7 ft/sec, 7.6 feet below the surface; and the maximum measured ebb velocities was 3.9 ft/sec, 5.1 feet below the surface.

The flows computed using the velocity data show that maximum flood flow rates at the south inlet are 60% of the total maximum flood flow rate through both inlets. The total peak flood discharge rate of both inlets is similar to what was measured in 2004 at the south inlet, approximately 94,800 $ft^3$/sec measured in 2004 versus 99,500 $ft^3$/sec measured in 2007. The predicted offshore tide range during the flooding tide of the November 16, 2004 survey was 7.9 feet, compared to 5.5 feet on November 14, 2007.

Therefore, the flood tide range was 30% smaller for the 2007 survey, but the measured discharges were nearly equal.

During the ebbing portion of the tide cycle, maximum flow rates through the south inlet are 70% of the total maximum ebb flow through both inlets. Similar to the flood tide results, the maximum ebb tide flow rate measured in 2004 is approximately equal to the total flow through both inlets in 2007, where 69,700 $ft^3$/sec was measured in 2004 and 71,900 $ft^3$/sec was measured in 2007. The predicted offshore tide range during the ebbing tide of the November 16, 2004 survey was 8.7 feet, compared to 6.3 feet on November 14, 2007. Again, similar to the measured flood tide results, the ebb tide range was 28% smaller for the 2007 survey, but the maximum measured ebb discharges were nearly the same. As expected, this trend indicates that the estuarine system with the north breach is more hydraulically efficient, allowing a greater tidal prism than the pre-breach conditions. The tidal measurements also illustrate this trend, where the larger post-breach tides observed at the fish pier and Meetinghouse Pond indicate an increase in overall tidal prism.

## 3. HYDRODYNAMIC MODEL

The Pleasant Bay RMA-2 model mesh developed for the 2006 MEP (Howes, *et al*., 2006) report was modified to include the new north inlet and updated bathymetry from the 2007 LIDAR survey. A detail of the modified grid is shown in Figure 3. The survey coverage included Chatham Harbor and a large swath of the eastern portion of Pleasant Bay, to depths greater than -20 ft, NGVD. The updated model mesh has 2677 quadratic elements with 7545 corner and mid-side nodes.

### 3.1 Calibration

The model was recalibrated using the tide data collected at three stations during the November 2007 deployment period. For the calibration, the model was run for a 198-hour period starting November 12 at 13:00 EST. This time includes a 24 hour model ramp-up period plus 14 $M_2$ tide cycles (each 12.42 hours long). Alterations made to the model calibration parameters used in the model of 2004 conditions included the addition of a new material type for the area of the new north inlet (new material type 28 with a friction factor of 0.030) and changes to the friction factor applied to the area of the south inlet (material type 1 changed from 0.027 to 0.030, material type 2 changed from 0.028 to 0.025).

Figures 4 through 6 show a comparison of model output and the measured tide. A tabulation of tide constituent amplitudes and phases for the simulation period is presented in Table 3, for both the measured data and model output. The model error is also shown in this table. The amplitude error is generally of the order 0.01 feet for the two gauges inside the system (i.e. at the fish pier and Meetinghouse Pond) while the maximum errors are still smaller than the accuracy of the tide data recorders (approximately 0.1 feet). Maximum constituent phase errors are within two model time steps (the same time step of the data).

### 3.2 Verification

An independent verification of the model's accuracy was made by comparing flow rates computed by the model to rates computed using the data from the ADCP survey. Flow rates in the model were computed along continuity lines specified in the model that follow the same paths used during the ADCP survey (Figure 1). Plots showing measured and modeled flow rates are shown in Figure 7 for the north inlet and Figure 8 for the south inlet. The comparison is very good at both ADCP transects, with calculated $R^2$ correlation coefficients greater then 0.94, and RMS errors of approximately 10% of the maximum measured flow rates.

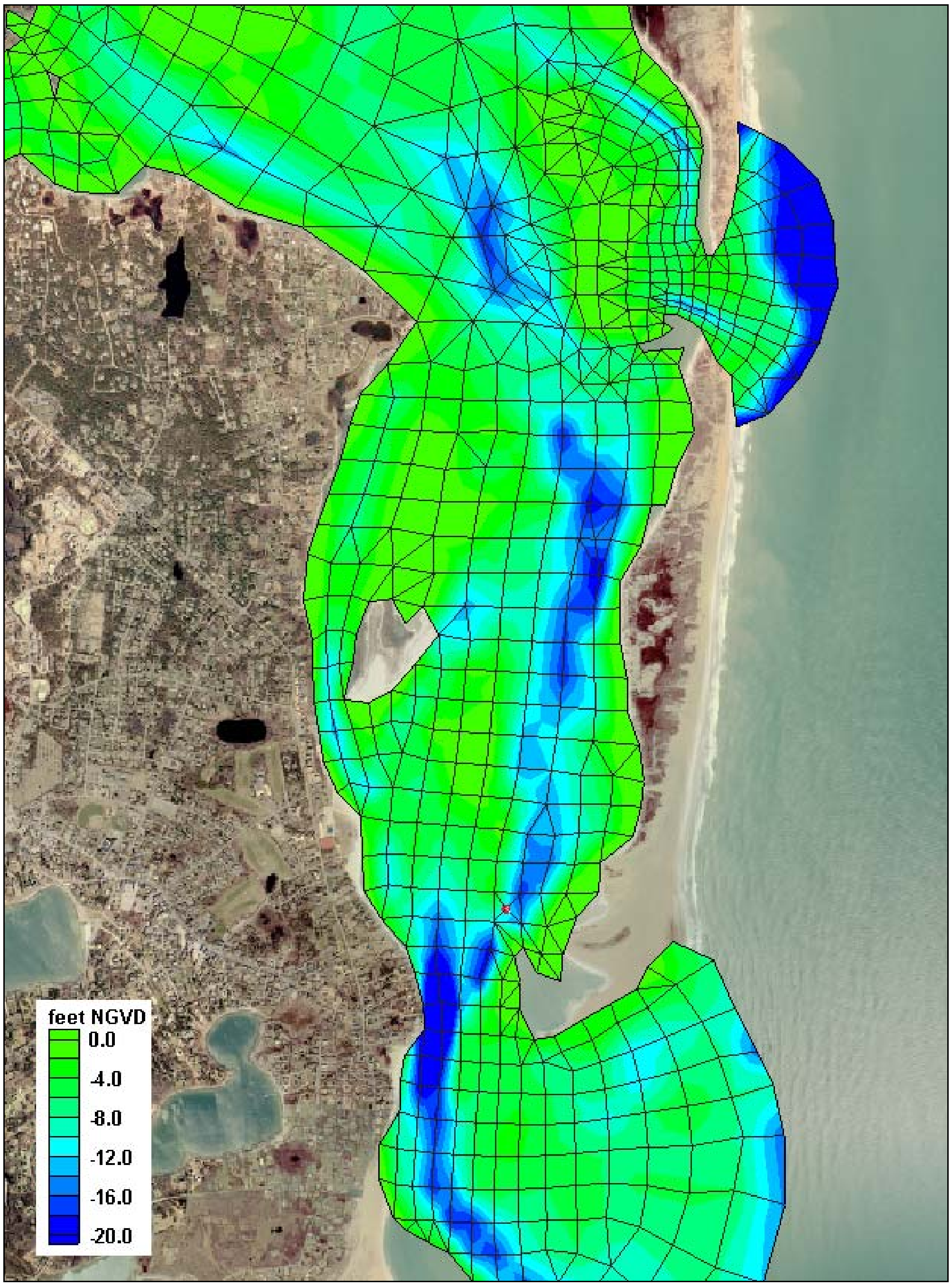


Figure 3. Detail of model grid of November 2007 conditions of Pleasant Bay, showing bathymetry contours and grid mesh at the north and south inlets.

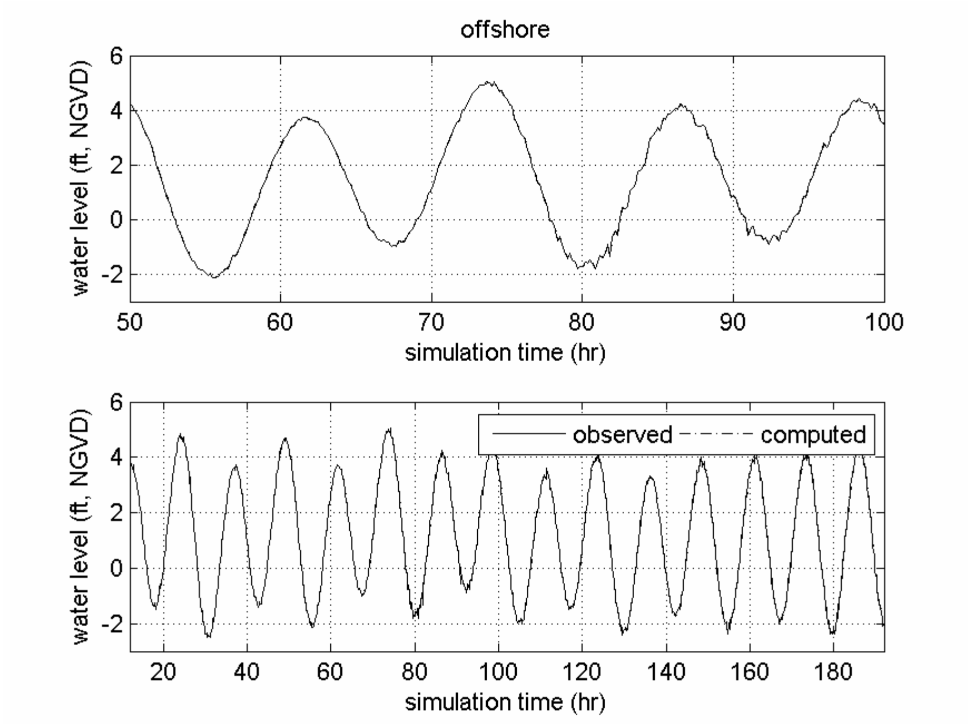


Figure 4. Comparison of model output and measured tides for the TDR location offshore Nauset Beach and the inlets to Pleasant Bay. The top plot is a 50-hour sub-section of the total modeled time period, shown in the bottom plot.

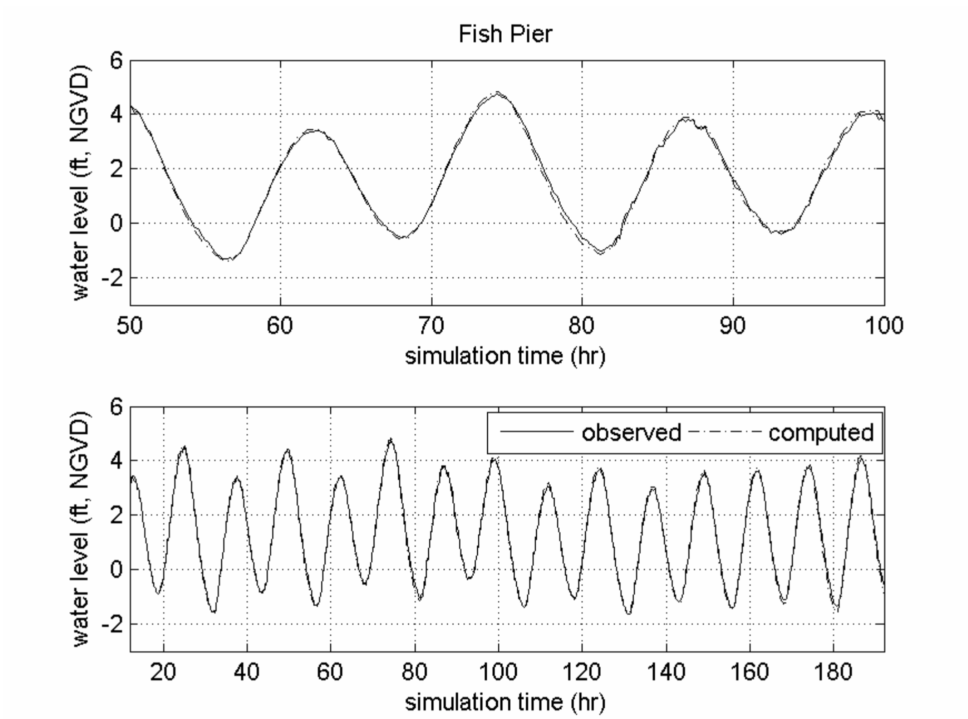


Figure 5. Comparison of model output and measured tides for the TDR station at the Chatham Fish Pier. The top plot is a 50-hour sub-section of the total modeled time period, shown in the bottom plot.

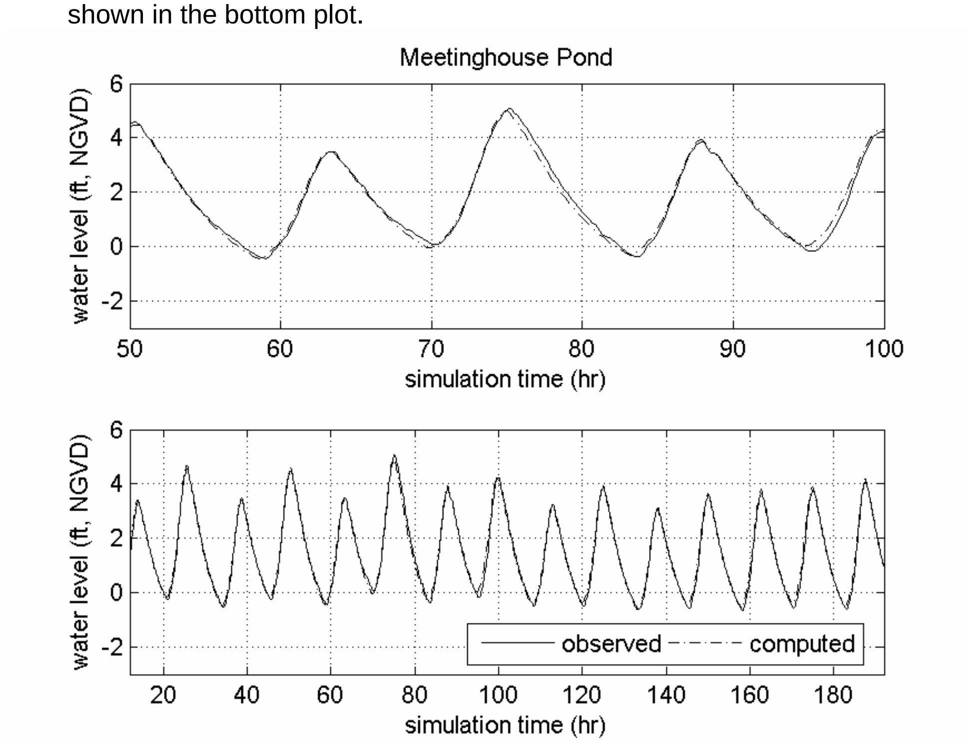


Figure 6. Comparison of model output and measured tides for the TDR station in Meetinghouse Pond. The top plot is a 50-hour sub-section of the total modeled time period, shown in the bottom plot.

Table 3. Tidal constituents for measured tide data and calibrated model output, with model error amplitudes, for the Pleasant Bay system, during modeled November 2007 calibration time period.

| Model calibration run | | | | | | |
|---|---|---|---|---|---|---|
| Location | Constituent Amplitude (ft) | | | | Phase (deg) | |
| | $M_2$ | $M_4$ | $M_6$ | $K_1$ | $\phi M_2$ | $\phi M_4$ |
| Offshore | 2.86 | 0.04 | 0.03 | 0.58 | 283.2 | 295.1 |
| Chatham Fish Pier | 2.43 | 0.08 | 0.07 | 0.50 | 298.6 | 161.3 |
| Meetinghouse Pond | 1.85 | 0.40 | 0.08 | 0.45 | 343.4 | 269.2 |
| **Measured tide during calibration period** | | | | | | |
| Location | Constituent Amplitude (ft) | | | | Phase (deg) | |
| | $M_2$ | $M_4$ | $M_6$ | $K_1$ | $\phi M_2$ | $\phi M_4$ |
| Offshore | 2.86 | 0.03 | 0.03 | 0.59 | 285.0 | 313.3 |
| Chatham Fish Pier | 2.34 | 0.08 | 0.07 | 0.49 | 302.5 | 148.0 |
| Meetinghouse Pond | 1.87 | 0.44 | 0.07 | 0.49 | 349.0 | 278.0 |
| **Error** | | | | | | |
| Location | Error Amplitude (ft) | | | | Phase error (min) | |
| | $M_2$ | $M_4$ | $M_6$ | $K_1$ | $\phi M_2$ | $\phi M_4$ |
| Offshore | 0.00 | -0.01 | 0.00 | 0.01 | 3.9 | 18.4 |
| Chatham Fish Pier | -0.08 | 0.00 | 0.00 | -0.01 | 8.2 | -13.9 |
| Meetinghouse Pond | 0.02 | 0.04 | -0.01 | 0.00 | 11.7 | 9.1 |

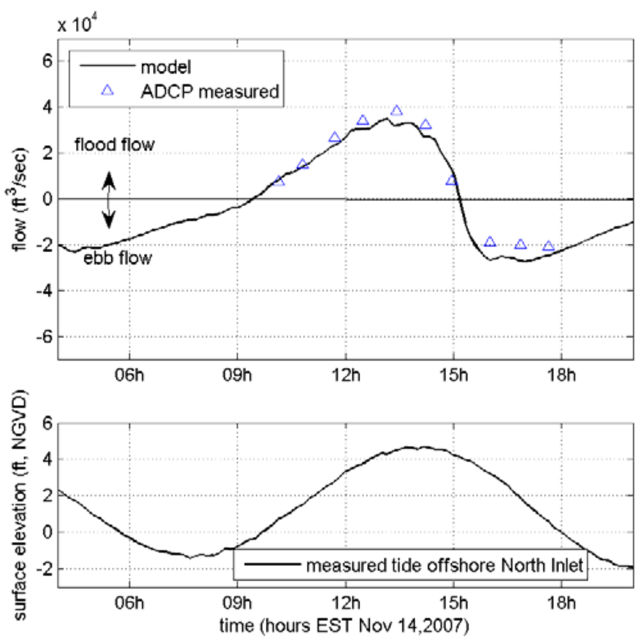


Figure 7. Comparison of measured volume flow rates versus modeled flow rates (top plot) through the north inlet over a tidal cycle November 14, 2007. The computed RMS error for this model run was 5,400 $ft^3$/sec, with an $R^2$ correlation coefficient of 0.94. Flood flows into the inlet are positive (+), and ebb flows out of the inlet are negative (-). The bottom plot shows the tide elevation offshore Nauset Beach.

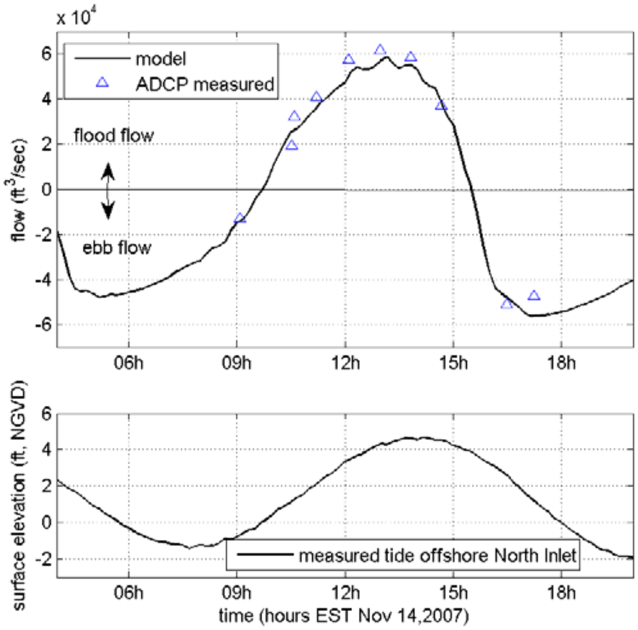


Figure 8. Comparison of measured volume flow rates versus modeled flow rates (top plot) through the south inlet over a tidal cycle November 14, 2007. The computed RMS error for this model run was 6,300 $ft^3$/sec, with an $R^2$ correlation coefficient of 0.98. Flood flows into the inlet are positive (+), and ebb flows out of the inlet are negative (-). The bottom plot shows the tide elevation offshore Nauset Beach.

A large portion of the error is due to assumptions used in the calculation of flow rates computed using the ADCP velocity measurements. Estimates of flow are required for the surface and bottom layers of the water column that are not directly measured by the ADCP. In this survey, the first measurement cell of the ADCP was 3.5 feet below the surface. To calculate the discharge rate across the ADCP transect line, the flows in the top and bottom layers are estimated using the nearest velocity measurements in the water column.

### 3.3 Flow Characteristics

The calibrated hydrodynamic model is a useful tool that is an extension of the physical data used in its development. The model can be used to examine the hydrodynamic characteristics of the system in areas or for times where no physical data exist.

Figures 9 and 10 show contour maps of depth averaged velocities modeled at maximum ebb and flood currents, respectively. Both of the plots represent a single model time step taken from the complete model simulation period. In the vicinity of the north inlet, maximum depth averaged velocities are 5.0 ft/sec during ebb tide, and 5.5 ft/sec during flood tide. For the area of the south inlet, the maximum computed ebb velocity is 5.8 ft/sec, and a maximum of 3.5 ft/sec for all flooding tides during the simulation. These results are not directly comparable to the measurements made by the ADCP, since the model output are depth averaged, and sampled from an area with a greater geographical extent than the ADCP transect lines.

A residual analysis of tidal flows was performed to determine if flows are split differently between the two inlets during the flood and ebb portions of the tide cycle. The flood and ebb tide prisms were computed for each inlet and averaged over the 14 tide cycles of the model simulations. These calculations are based on flow rates taken from the model along transects at the north inlet and the northern limit of Chatham Harbor (between Allen Point and Nauset Beach). The flood (+) and ebb (-) prisms where added together to determine the average tidal residual for the simulation period. The results are presented in Table 4.

Table 4. Computed average flood and ebb tide prisms (in cubic feet) of Pleasant Bay, and resulting residual flows for the north inlet and south inlet channel.

| | North Inlet | South Inlet |
|---|---|---|
| Flood Tide | 377,796,000 | 566,783,000 |
| Ebb Tide | 335,416,000 | 608,670,000 |
| Residual (f-e) | 42,380,000 | -41,887,000 |

The residual analysis indicates that there is a small residual flow equal to 4.5 % of the total prism of both inlets together. At the north inlet, the average flood tide prism is 42 million cubic feet (MCF) larger than the ebb tide prism. It is the opposite case for the south inlet. Though the flows are greater in the south inlet channel, the residual flow is essentially the same (42 MCF), though it is the ebb tide prism that is larger. This simply indicates that on average 42 MCF of the total prism of the system enters the Pleasant Bay system though north inlet but is discharged through the south inlet.

Based on the spatial distribution of maximum current velocities shown in Figures 9 and 10, the slight residual influences the tidal current distribution and may have alter the associated sediment transport patterns. Specifically, a comparison of Figure 9 (maximum ebb currents) and Figure 10 (maximum flood currents) illustrates the dominance of strong ebb currents through the main navigation channel in the south inlet for the region north of the Chatham Lighthouse. The weaker flood current through the south inlet has potentially reduced further development of the flood shoal in the vicinity of Tern Island. In contrast, the larger flood currents immediately landward of the north inlet entrance illustrate the driving force likely responsible for development of the flood shoal complex in this region.

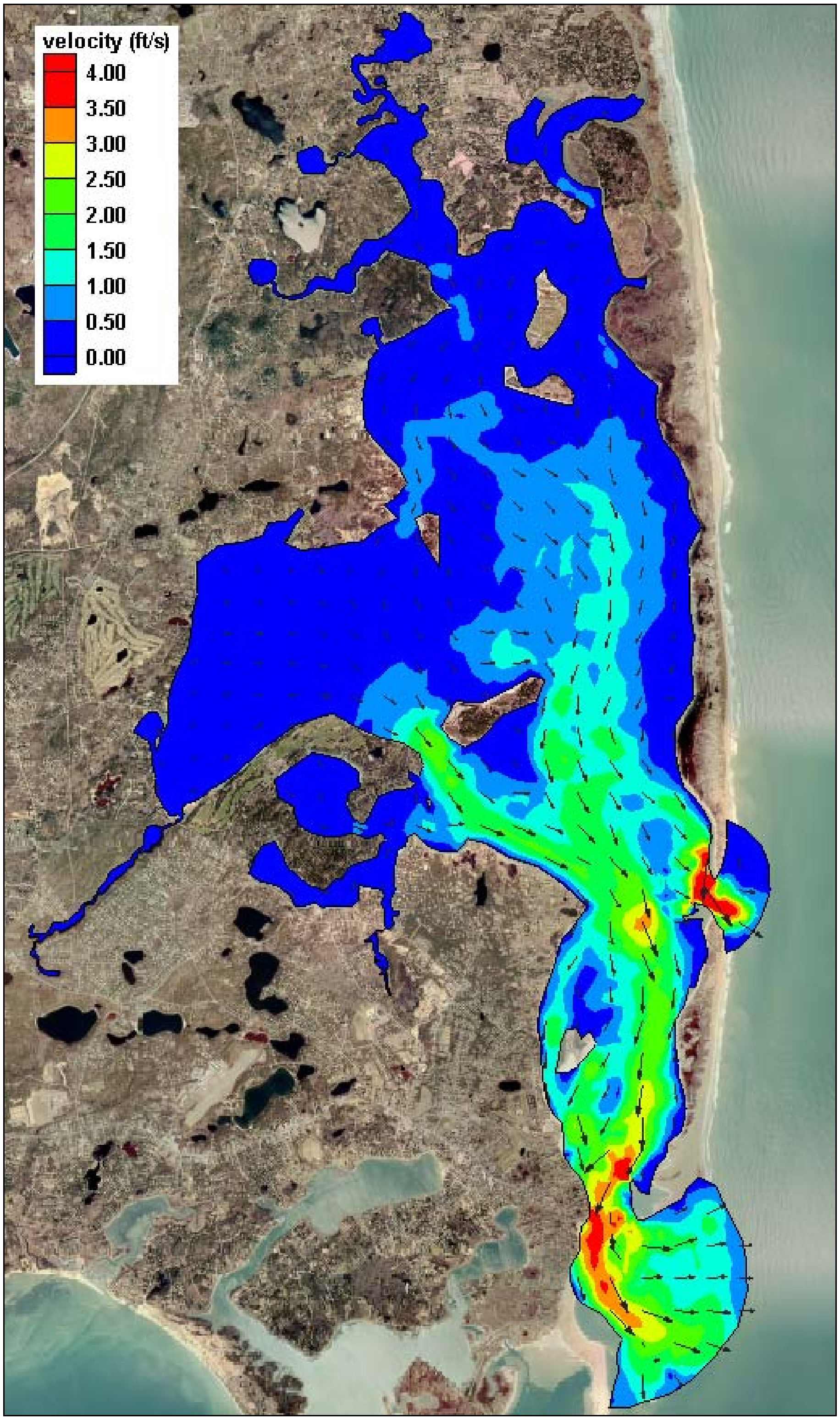


Figure 9. Contour plot with vectors of maximum ebb currents during November 2007 simulation period.

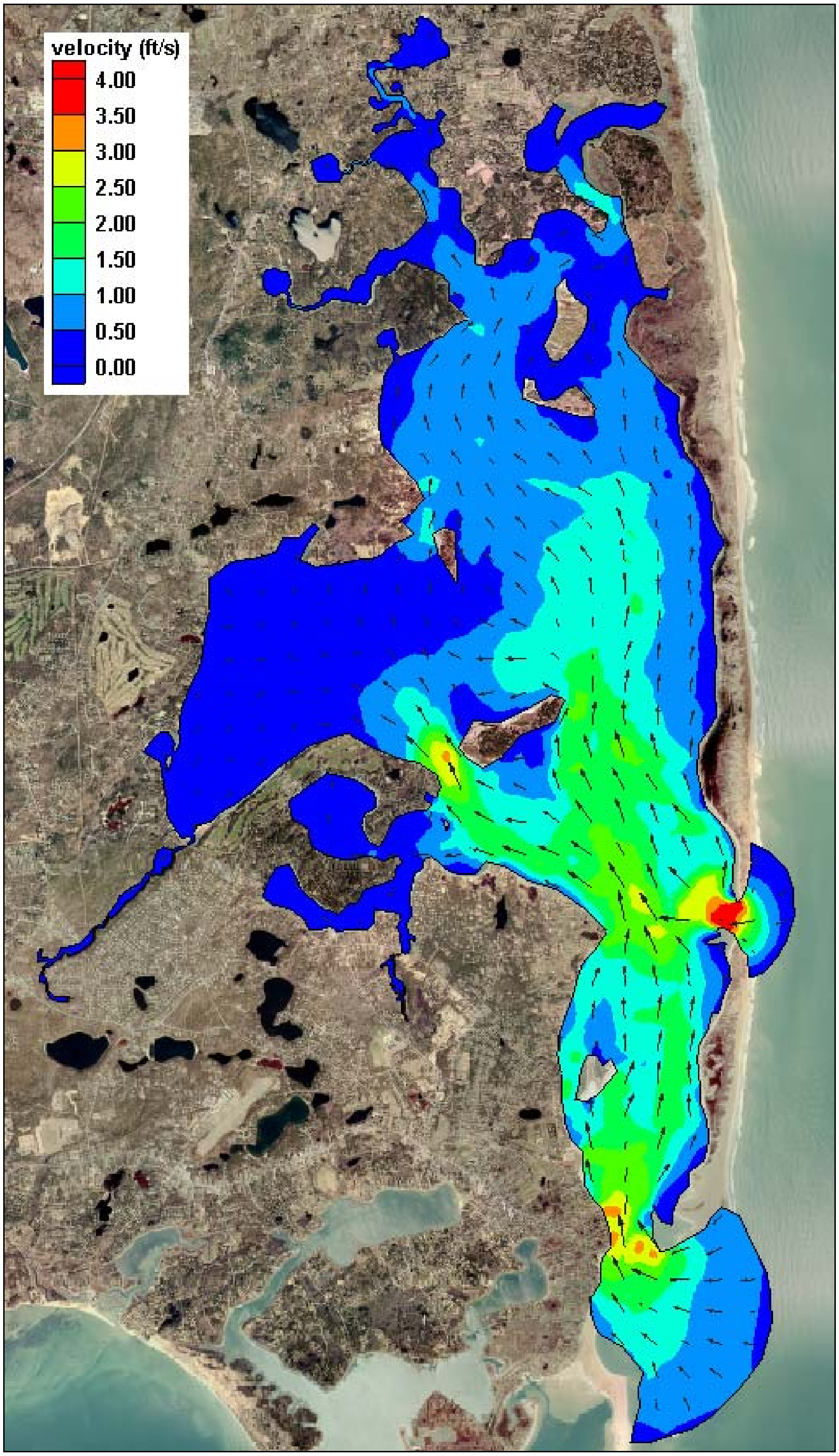


Figure 10. Contour plot with vectors of maximum flood currents during November 2007 simulation period.

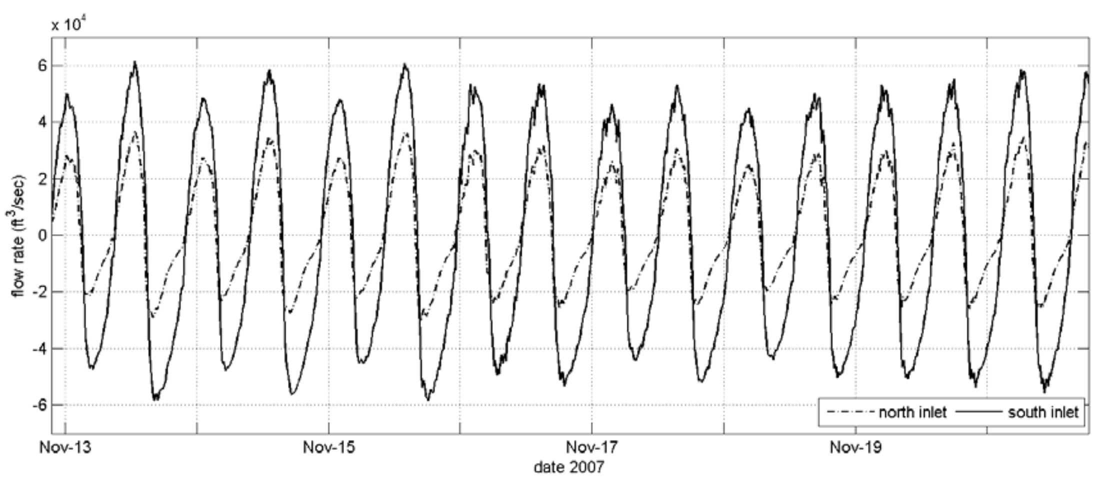


Figure 11. Modeled flow rates across ADCP transect line A1 (north inlet) and A2 (south inlet) during calibration time period (198 hours).

## 4. COMPARISON TO 2004 CONDITIONS

A direct comparison of pre- and post-breach hydrodynamic conditions in Pleasant Bay is possible by running the pre- and post-breach model grids using the same offshore tidal open boundary condition. By driving both models with the same offshore tide, biases in the measured data that occur because of time period differences are eliminated. This is a powerful utility of hydrodynamic models, since this is not a possibility with the real physical system.

A comparison of tides in Meetinghouse Pond is shown in Figure 12, for modeled 2004 pre-breach and 2007 post-breach conditions. Both scenarios were driven with the same November 2007 tide used in the calibration of the post-breach model. The average tide range during the simulation period is 3.6 feet pre-breach, and 4.3 feet post-breach, which is a 0.7 foot or 19.4% increase in the average tide range of the pond from 2004 to 2007.

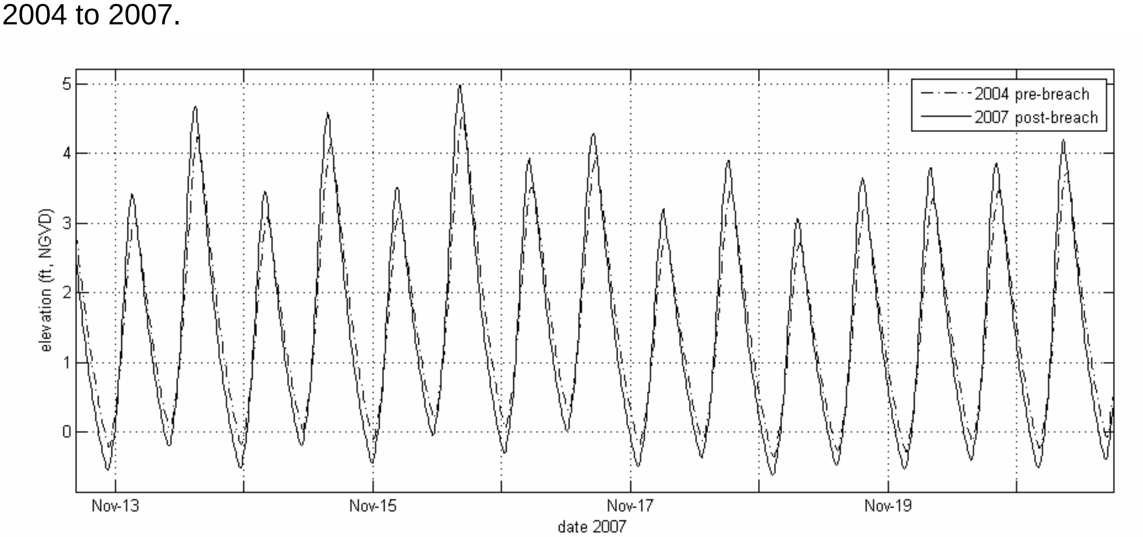


Figure 12. Comparison of tides in Meetinghouse Pond from the simulation of modeled 2004 pre-breach and 2007 post-breach conditions.

Figure 13 compares flow rates of the 2004 and 2007 models. The 2004 flow rates were computed in the model across a continuity line placed across the boundary between Chatham Harbor and Pleasant Bay, at Allen Point. The 2007 flow rates were computed using a continuity line placed at the same location from Allen Point, and a second line placed across the throat of the north inlet.

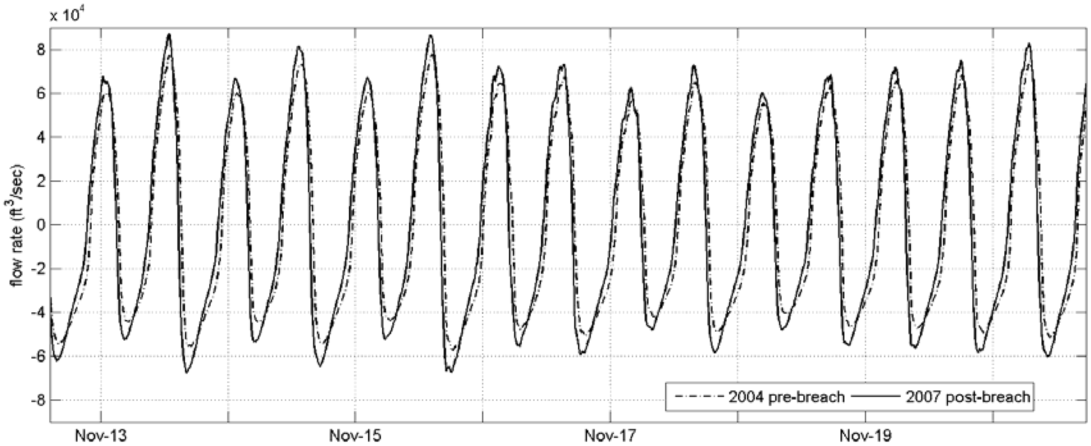


Figure 13. Total modeled flow rates flooding to and ebbing from the main basin of Pleasant Bay (not including Chatham Harbor), simulated using the 2004 pre-breach model and 2007 post-breach model. Both simulations used the same November 2007 offshore tide to drive the model.

Average tide prisms of Pleasant Bay and its connected sub-embayment systems (including Chatham Harbor) were computed for both pre- and post-breach conditions, using the computed flow rates. The average post-breach prism (based on flood tides) during the November 2007 simulation period was computed to be 1,147.0 MCF. For the pre-breach simulation, the average flood prism was computed to be 998.5 MCF. Therefore, the tidal prism increased by 14.9% between the 2007 post-breach and 2004 pre-breach conditions. The total prism exchanged through the south inlet has decreased 24% between the 2004 and 2007 modeled conditions.

Contour plots of velocity magnitude are shown in Figures 14 and 15 for pre-breach inlet conditions, for maximum ebb and flood currents computed using the offshore November 2007 tide to drive the open boundary. A comparison of the modeled currents with post-breach conditions (Figures 9 and 10) shows that the south inlet has experienced a significant reduction in tidal currents as a result of the north inlet formation.

Change plots that quantify the magnitude of the velocity change between 2004 and 2007 are presented in Figures 16 and 17. For these plots, the velocity fields computed for a single time step from maximum flood and ebb tide of the 2004 simulation were subtracted from the time of maximum currents computed for the 2007 model simulation. The greatest reduction in tidal currents for both the ebb and flood portions of the tide is along the face of the revetments protecting Watch Hill Way and Holway Street residences. This region of south inlet has the deepest bathymetry in the Chatham Harbor/Pleasant Bay system; however, the significant reduction in tidal currents at this location should enhance sedimentation. In addition, a significant reduction in tidal current velocities also extends from the Holway Street revetments, across the inlet channel to Nauset Beach. Since this area represents the region historically scoured following the 1987 breach, the modeled reduction in currents through this portion of the south inlet likely would lead to temporary stability of the channel. As shown in Figure 18, the existing conditions are reminiscent of the 1870-1890 timeframe described by Geise (1988). If the Chatham Harbor system follows the historic pattern that followed the 1846 breach, relatively rapid landward migration of the barrier beach system can be anticipated for the area south of the north inlet, as shown in Figure 18.

Overall, the modeling shows that the 2007 breach caused a general reduction in maximum tidal currents throughout Chatham Harbor (the blue shaded areas of Figures 16 and 17). This reduction in velocities likely will alter the location of shoals as sediment entering and exiting the south inlet readjusts currents that mobilize and transport the material. For both the flood and ebb shoal, the areas of accretion will likely migrate closer to the inlet area with the smallest cross-section (adjacent to the Watch Hill Way and Holway Street revetments). Accretion from flooding currents (i.e. the flood shoal) likely will occur south of the existing flood shoal. Accretion governed by the ebbing tide through the south inlet likely will occur in the shallow region of the existing bypass bar, since the reduction in tidal currents prevents transport of material further offshore. At this time, it is not clear how this reduction of tidal currents will influence the stability of the existing navigation channel through the bypass bar.

The formation of the north inlet in 2007 provided an increase in tidal exchange for the Chatham Harbor/Pleasant Bay system. As shown in Figures 16 and 17, the post-breach conditions represent an increase in tidal currents within much of Pleasant Bay for both maximum ebb and flood conditions. Within the vicinity of the new breach, the increase in tidal currents through the inlet throat and the reduction of these high currents led to the observed formation of well-defined flood and ebb shoals. As depicted in Figures 9 and 17, a significant increase in ebb tide currents along the western shoreline of the barrier system north of the new breach likely has been responsible for much of the observed shoreline erosion in this region. In general, the model indicates that the north inlet primarily services the Pleasant Bay portion of the estuarine system. The orientation of the developing tidal channels through this inlet also appears to support this hypothesis. As of November 2007, accretion associated with the north inlet shoals had no direct influence on the federal navigation channel to Aunt Lydia’s Cove.

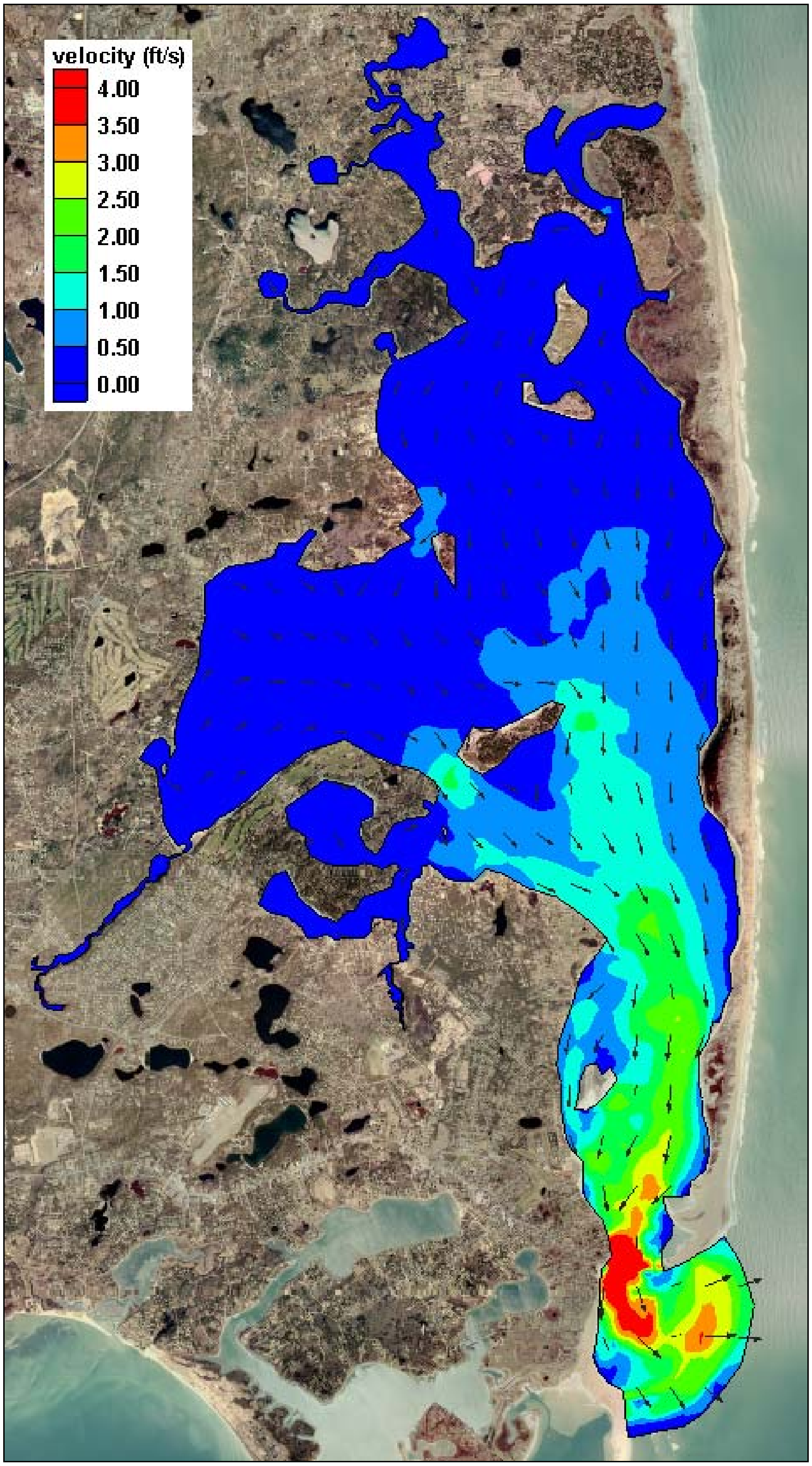


Figure 14. Contour plot with vectors of maximum ebb currents for pre-breach conditions, using November 2007 offshore tide.

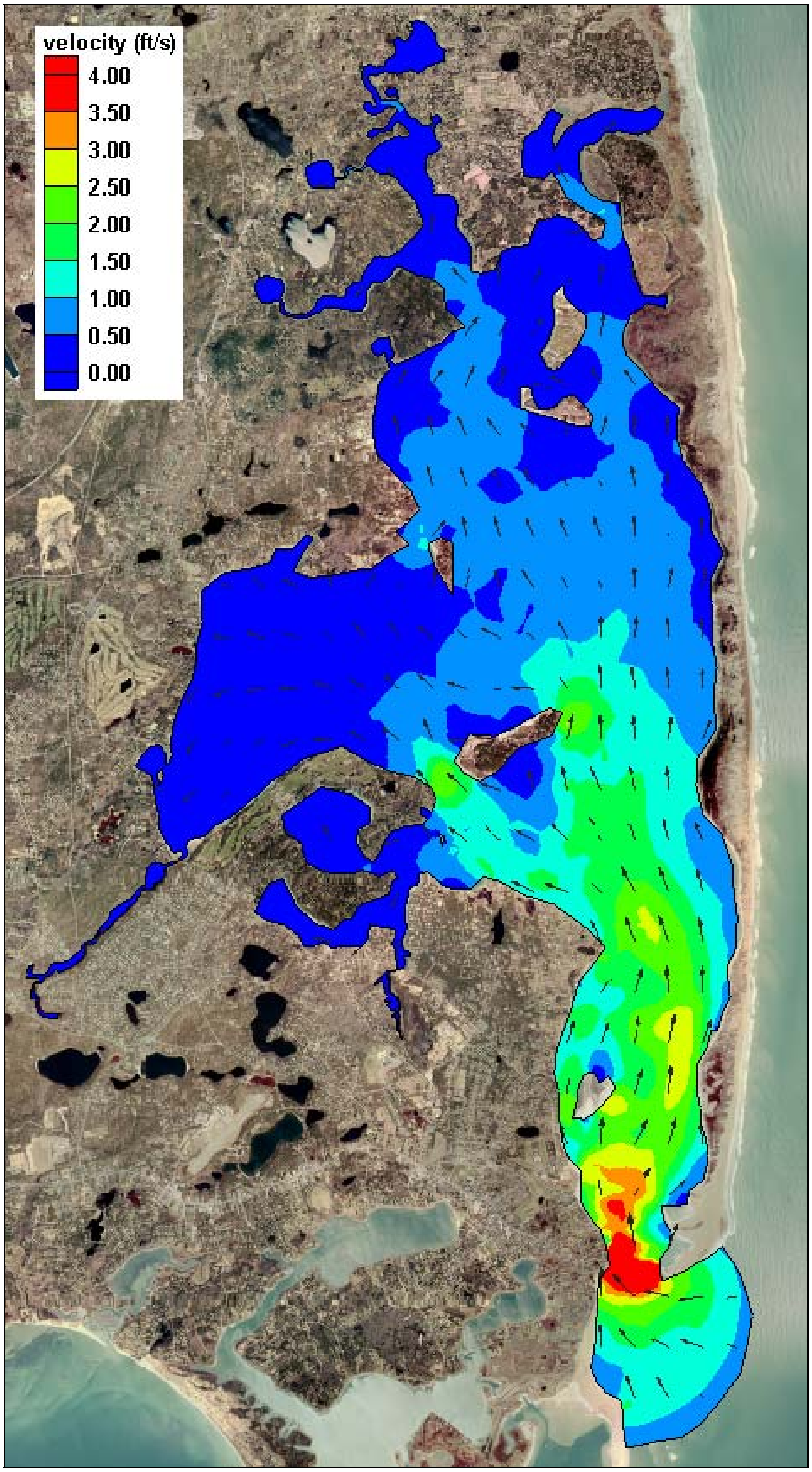


Figure 15. Contour plot with vectors of maximum flood currents for pre-breach conditions, using November 2007 offshore tide.

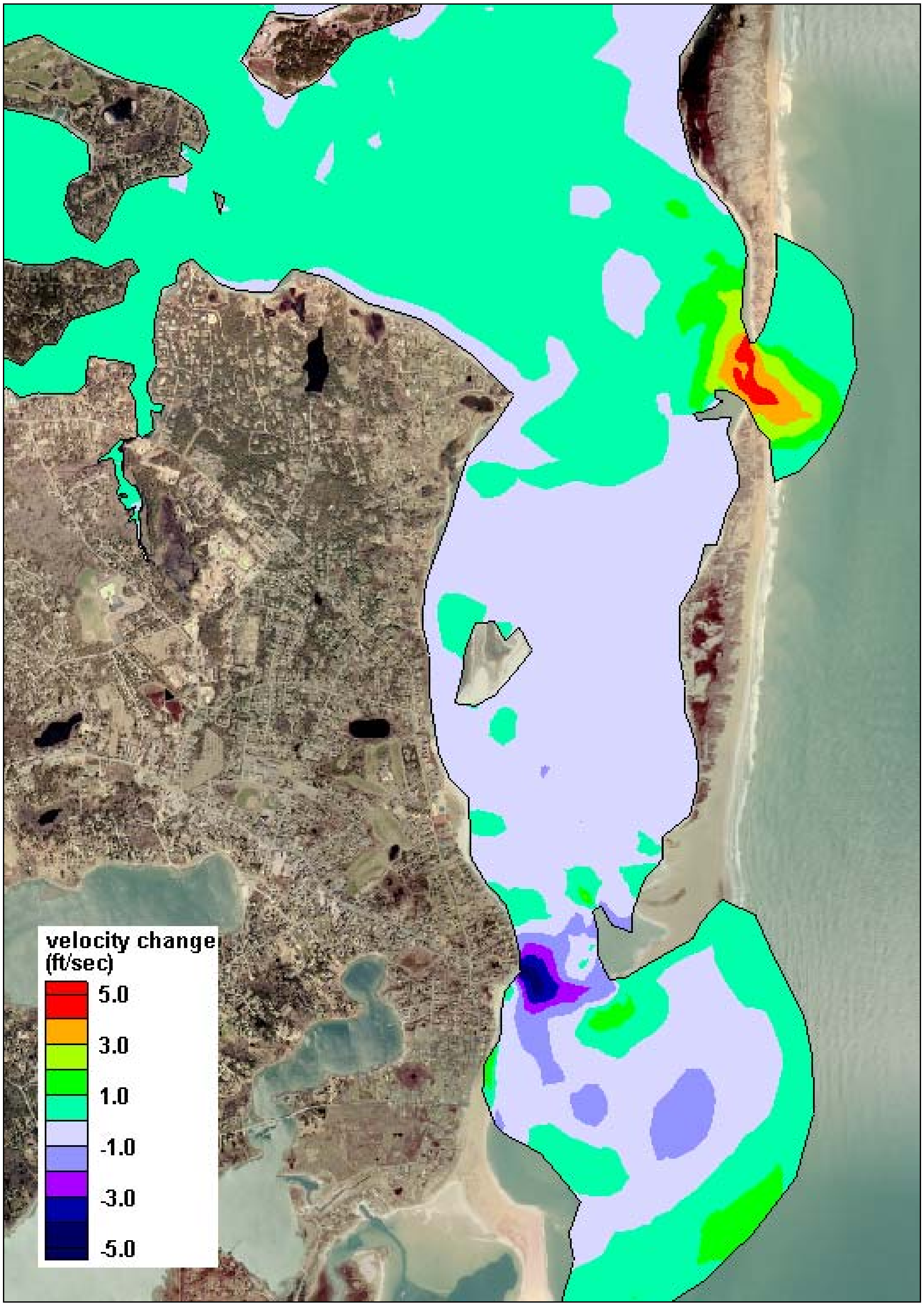


Figure 16. Contour plot showing computed maximum ebb velocity change (post minus pre) between model runs of 2004 and 2007 inlet configurations, both using the November 2007 offshore boundary condition.

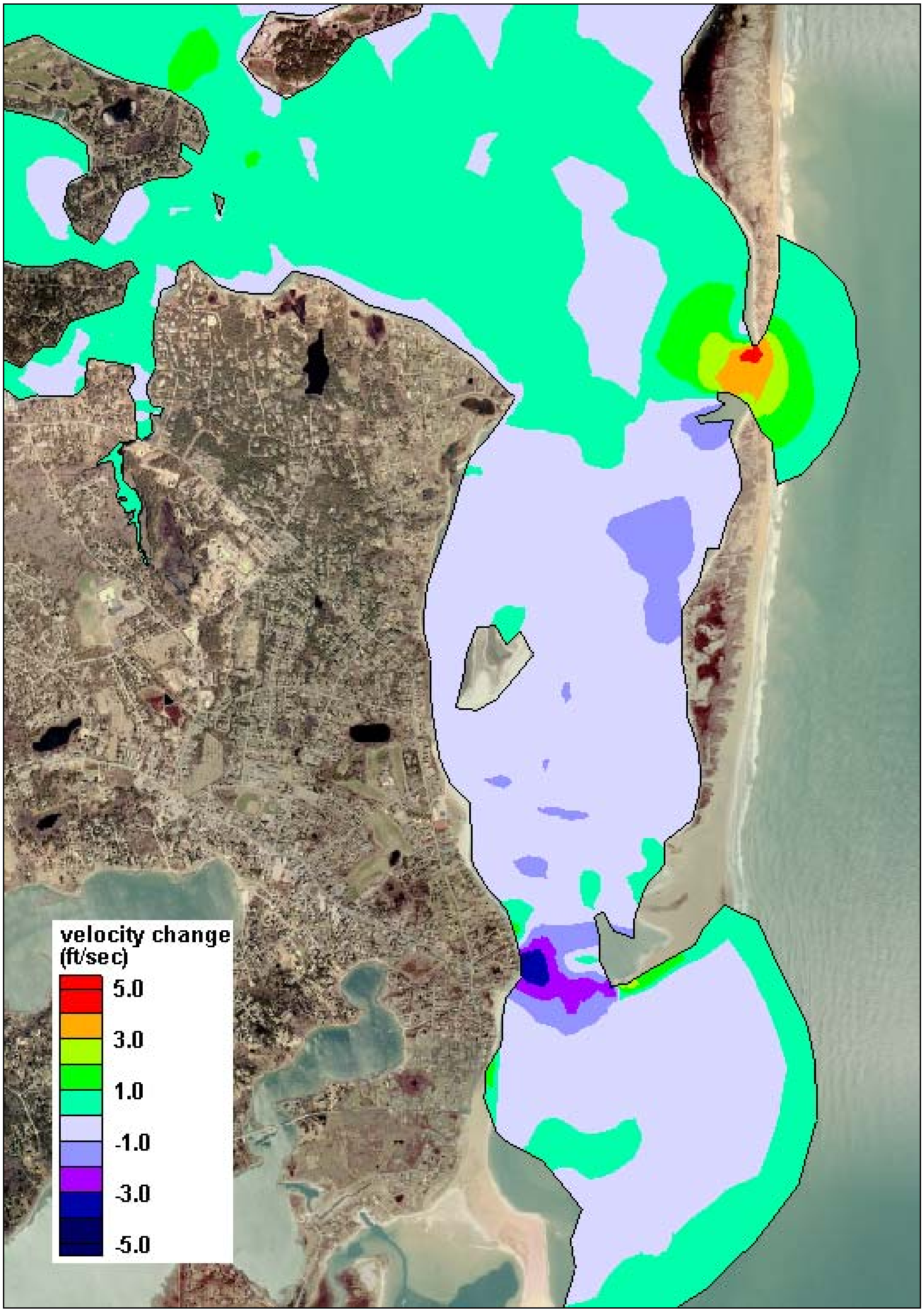


Figure 17. Contour plot showing computed maximum flood velocity change (post minus pre) between model runs of 2004 and 2007 inlet configurations, both using the November 2007 offshore boundary condition.

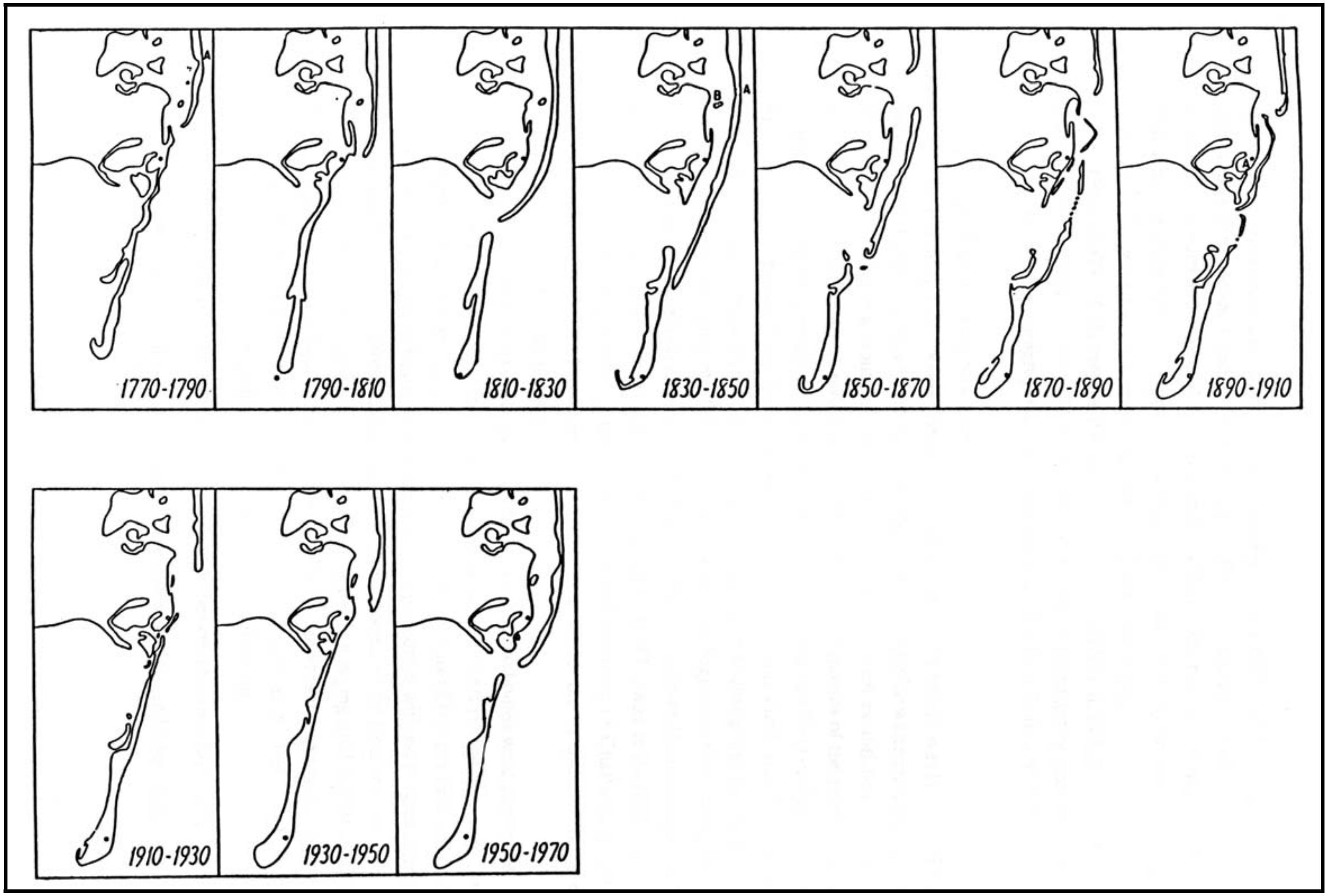


Figure 18. Historical changes in the Nauset Beach-Monomoy barrier system illustrated by generalized 20-year diagrams from 1770-1790 to 1950-1970 (from Geise, 1987).

## 5. **REFERENCES**

Geise, G.S. (1988). "Cyclical Behavior of the Tidal Inlet at Nauset Beach, Massachusetts: Application to Coastal Resource Management." In: Lecture Notes on Coastal and Estuarine Studies, Volume 29, Symposium on Hydrodynamics and Sediment Dynamics of Tidal Inlets (D. Aubrey and L. Weishar, eds.), Springer-Verlag, NY, pp. 269-283.

Howes B., S. W. Kelley, J. S. Ramsey, R. Samimy, D. Schlezinger, E. Eichner (2006). Linked Watershed-Embayment Model to Determine Critical Nitrogen Loading Thresholds for Pleasant Bay, Chatham, Massachusetts. Massachusetts Estuaries Project, Massachusetts Department of Environmental Protection. Boston, MA. 227pp. Available online at http://www.oceanscience.net/estuaries/